CLM-P725

CLM-P725

UKAEA

Preprint

MODELLING OF A TRANSPORT PROBLEM IN PLASMA PHYSICS

B. J. BRAAMS

CULHAM LABORATORY
Abingdon Oxfordshire

1984

CLM-P 725

MODELLING OF A TRANSPORT PROBLEM IN PLASMA PHYSICS

B.J. BRAAMS[2]

August, 1984

ABSTRACT

A two-dimensional, two-fluid model for transport processes in the edge plasma in a tokamak device is presented, and the numerical methods employed for its solution are described. Emphasis is given to those aspects of the numerical treatment which are generally relevant to the solution of coupled systems of convection–conduction equations.

[1]To appear in: "Topics in Applied Numerical Analysis" (J.G. Verwer, ed.), CWI Syllabus, Centrum voor Wiskunde en Informatica, Amsterdam, 1984.

[2]F.O.M. Instituut voor Plasmaphysica, Postbus 1207, 3430 BE Nieuwegein, The Netherlands. Present address: Max-Planck-Institut für Plasmaphysik, D-8046 Garching bei München, Fed. Rep. Germany.

INTRODUCTION

An important problem in plasma physics for nuclear fusion is how to extract from the magnetic confinement device the large amounts of energy and alpha particles which are produced in the inner plasma. In the interior of the toroidal confinement region the main transport process is diffusion across magnetic surfaces, while near the edge it is flow along those field lines that intersect a material boundary [1]. Until recently these two processes were only modelled separately, with sophisticated codes for the one-dimensional radial transport problem, and fairly crude models for the one-dimensional flow along the field lines.

The subject of this presentation is the two-dimensional two-fluid modelling of the edge plasma region [2], [3], where both the radial diffusion of particles and energy and the convection and conduction along field lines are important processes. A two-fluid model is employed because the electrons and the ions have separate (but coupled) energy balances. The code that has been developed for these studies is based on a finite-volume discretization of the conservation equations on a topologically rectangular mesh, using methods of D.B. Spalding's school [4]. The discretization is fully implicit in time with the aid of an elliptic pressure correction procedure. The discrete coefficients are a continuous function of the local cell Péclet number, with central differencing and pure convective upwind differencing as the appropriate limits. The equations are solved by a method based on incomplete L*U decomposition.

The paper is organized as follows. Section 1 presents a simplified version of the governing differential equations of our model. The simplified set exhibits all the essential features which are relevant to the choice of the numerical methods employed for the solution of the full set, while omitting most of the details. The full set of equations is given in appendix A. In section 2 the numerical methods are presented. We review the semi-implicit procedure of Patankar and Spalding, in which the continuity equation is replaced by an elliptic pressure correction equation, and their hybrid (central–upwind) discretization scheme for convection–conduction equations. Also discussed is our approach to the special problem of the coupling between the electron and the ion energy equations. In section 3 some calculations are shown.

The need for numerical solutions to coupled systems of convection–conduction equations arises in many branches of physics and engineering. The present paper is meant to be self-contained for an audience with an interest in computational fluid dynamics, but not neccesarily interested in the plasma physics context of our work. The governing equations are presented with a minimum of physical justification, and the generally relevant aspects of the numerical treatment are emphasized. Those who have a specific interest in the edge plasma modelling may consider this paper as a companion to [2] and [3].

1. A Two-Dimensional Model of the Edge Plasma

Physical description. In a magnetized plasma the charged particles are constrained, in lowest approximation, to follow helical orbits 'tied' to a magnetic field line. Parallel and perpendicular[1] transport processes therefore differ in character. Parallel transport of particles is governed by a momentum balance equation, and perpendicular transport by a diffusion equation. Energy transport is described by a convection–conduction equation in both directions, but the parallel conductivities are much larger than the perpendicular ones. In a magnetic confinement configuration of the tokamak type each magnetic field line is generally constrained to lie on a toroidal 'flux' surface, and it may be assumed that the density, the electron temperature and the ion temperature are each constant over a flux surface. The transport equations may then be reduced to a one-dimensional (perpendicular to the flux surfaces) set.

The assumption of uniformity along field lines breaks down in the edge region of the plasma, where the field lines intersect material boundaries. In an axisymmetric toroidal device the transport in this region requires a two-dimensional description.

Simplified mathematical model. An appropriate set of equations is made up of a continuity equation for the ion density n_i, a momentum balance equation governing the parallel velocity u, a diffusion equation for the perpendicular velocity v, and convection–conduction equations for the electron- and ion temperatures, T_e and T_i (expressed in energy units). The full set as solved in our code is given in Appendix A. Below, a simplified version is given, which will serve in the next section as a basis for the discussion of the numerical methods. Auxiliary physical quantities appearing in the equations are the electron density, $n_e = Z_i n_i$, the mass density, $\rho = m_i n_i$, and the pressure, $p = n_e T_e + n_i T_i$. The coordinates x and y correspond to the parallel and perpendicular directions respectively. The simplified equations are:

$$\frac{\partial}{\partial t} n_i + \frac{\partial}{\partial x}(n_i u) + \frac{\partial}{\partial y}(n_i v) = S_n \tag{1}$$

$$\frac{\partial}{\partial t}(\rho u) + \frac{\partial}{\partial x}\left(\rho u^2 - \eta_x^i \frac{\partial u}{\partial x}\right) + \frac{\partial}{\partial y}\left(\rho v u - \eta_y^i \frac{\partial u}{\partial y}\right) = S_{mu} - \frac{\partial p}{\partial x} \tag{2}$$

$$v = -D \frac{\partial}{\partial y}(\ln n_i) \tag{3}$$

$$\frac{\partial}{\partial t}\left(\frac{3}{2} n_e T_e\right) + \frac{\partial}{\partial x}\left(\frac{5}{2} n_e u T_e - \kappa_x^e \frac{\partial T_e}{\partial x}\right) + \frac{\partial}{\partial y}\left(\frac{5}{2} n_e v T_e - \kappa_y^e \frac{\partial T_e}{\partial y}\right) = S_E^e - K_{ei}(T_e - T_i) \tag{4}$$

[1] The adjective 'parallel' refers to a component along the magnetic field, and 'perpendicular' refers to a component which is transverse to the toroidal flux surfaces.

$$(5)\qquad \frac{\partial}{\partial t}\Big(\frac{3}{2}n_iT_i+\frac{1}{2}\rho u^2\Big)+\frac{\partial}{\partial x}\Big(\frac{5}{2}n_iuT_i+\frac{1}{2}\rho uu^2-\kappa_x^i\frac{\partial T_i}{\partial x}\Big)$$
$$+\frac{\partial}{\partial y}\Big(\frac{5}{2}n_ivT_i+\frac{1}{2}\rho vu^2-\kappa_y^i\frac{\partial T_i}{\partial y}\Big)=S_E^i+K_{ei}\,(T_e-T_i)$$

S_n, S_{mu}, S_E^e and S_E^i are volume sources of ions, momentum, electron and ion energy. η_x^i and η_y^i are the parallel and perpendicular ion viscosities, $\kappa_x^{e,i}$ and $\kappa_y^{e,i}$ are thermal conductivities, D is the diffusivity, and K_{ei} is the energy equipartition coefficient. The source terms are complicated non-local functions of the sought solution, involving models for particle ionization and recombination, and for radiation energy loss. The transport coefficients are nonlinear local functions of the solution.

In this simplified set of equations the distinction between the parallel direction and the poloidal direction has been ignored, the equations have been written in a cartesian coordinate system instead of in a curvilinear orthogonal system, and some contributions have been left out of the energy equations. These aspects do not influence the numerical procedure in a significant way.

Boundary conditions. Counting derivatives, one sees that a total of seven conditions is required on the boundaries perpendicular to the x-coordinate; eight conditions are required on boundaries perpendicular to the y-coordinate. On each segment of the boundary there will be two conditions related to the energy equations, (4) and (5), specifying either an energy flux, or a temperature, or more generally specifying the energy fluxes in terms of the temperatures and density. For the parallel momentum equation we usually have a sonic flow specification on one face, and zero flow or zero shear elsewhere. For the continuity equation and the diffusion equation together, on one face perpendicular to the x-direction and on both faces perpendicular to the y-direction either the density, or the particle flux, or some combination of the two may be specified.

2. Numerical Treatment

Outline. Following [4] it was decided to employ a finite-volume spatial discretization on a staggered mesh, and a fully implicit discretization in time. Interest is in fact restricted to steady state solutions. The continuity equation is treated by the Patankar–Spalding implicit method [5], through which it is replaced by a pressure correction equation of standard convection–conduction form. The discrete coefficients for each of the convection–conduction equations are computed using the power law scheme of Patankar [4]; this is formally second-order accurate, and is stable at all values of the cell Péclet (or Reynolds) number. The resulting five-point equations are relaxed separately in a cyclic order; the Strongly Implicit Procedure (SIP) of Stone [6] is employed. The strong coupling between the two energy equations is eliminated by relaxing in turn the total energy and the ion energy balance. The following subsections present more details on the numerical methods.

Pressure correction procedure. The need for a special treatment of the continuity equation may be seen most clearly by consideration of incompressible flow. If one would consider the momentum equation (or, in our case, one component of the momentum equation, supplemented by a diffusion equation) to govern the velocity field, and the energy equation(s) to govern the temperature(s), then the continuity equation would have to govern the pressure. But the pressure does not even appear in that equation.

For compressible flow, the pressure is a derived quantity, and the density is one of the primary variables. The continuity equation as it stands then appears suitable for relaxation of the density field, but severe problems appear with low Mach number flows, when the fluid is effectively incompressible. The traditional prescription (e.g. [7]), is to employ an explicit discretization in time for the continuity equation, regardless of the treatment of the other equations in the system, with a time step governed by the CFL condition based on the velocity of sound.

Patankar and Spalding's method is to satisfy the continuity equation through simultaneous changes to the density, pressure, and velocity fields. We present the method here with reference to a steady-state equation of the form $\partial(nu)/\partial x + \partial(nv)/\partial y = S_n$, noting that it is equally well applicable to an implicit treatment of a time-dependent equation. At each iteration on the continuity equation the following coupled adjustments are made:

$$\text{(6)} \qquad \begin{cases} p := p + \xi \\ n := n + \kappa\xi \\ u := u - c_x \dfrac{\partial \xi}{\partial x} \\ v := v - c_y \dfrac{\partial \xi}{\partial y} \end{cases}$$

Inserting these changes into the continuity equation, and neglecting terms quadratic in ξ, one sees that ξ is to be obtained as solution to a standard convection–conduction equation:

$$\text{(7)} \qquad \frac{\partial}{\partial x}(\kappa u\xi - nc_x \frac{\partial \xi}{\partial x}) + \frac{\partial}{\partial y}(\kappa v\xi - nc_y \frac{\partial \xi}{\partial y}) = r$$

where r is the current residual, $r = S_n - \mathbf{div}\,(n\mathbf{u})$.

The coefficients κ, c_x, and c_y are choosen so as to minimize the damage that Eq. (6) does to the equation of state and to the equations governing the velocities. Obviously $\kappa := (\partial n/\partial p)_T$ is appropriate. The choice of the coefficients c_x and c_y is more difficult, and requires consideration of the discretized momentum equations. The discrete

equation for the x-velocity u has the form

$$A \cdot u = S_{mu} - \frac{\partial p}{\partial x} \tag{8}$$

We assume that A is a diagonally dominant operator of five-point form, and that everything which does not fit into A has been moved into the right hand side. The prescription of Patankar and Spalding for the coefficient c_x is now to set $c_x := 1/\alpha$ at each point, where α is the diagonal coefficient in the matrix A. In this way the adjustment $u := u - c_x \partial\xi/\partial x$ approximately cancels the effect of $p := p + \xi$ in the x-component of the momentum equation. With the usual fluid flow problems the prescription for c_y is similar, but in the system (1)–(5) the y-velocity is governed by a diffusion equation, leading immediately to the assignment $c_y := \kappa D/n$.

This implicit pressure correction procedure is also discussed by Brandt, e.g. [8], in a more general setting. There the method is referred to as 'distributive relaxation', and is recommended generally as a relaxation procedure for systems of equations which are not separately elliptic: the Cauchy–Riemann system, compressible and incompressible Navier–Stokes, and the Euler equations.

Spatial discretization. This section deals with the discretization scheme for a convection–conduction equation in conservation form:

$$\mathcal{L}\phi \equiv \mathbf{div}\,(\rho \mathbf{u}\phi - \mathbf{\Gamma} \cdot \mathbf{grad}\,\phi) = S \tag{9}$$

The differential operator is expanded on coordinates, and it is assumed that $\mathbf{\Gamma}$ is then diagonal, so that

$$\mathcal{L}\phi = \frac{1}{\sqrt{g}} \sum_{\alpha} \frac{\partial}{\partial x_\alpha} \Big(\frac{\sqrt{g}}{h_\alpha} \big(\rho u_\alpha \phi - \frac{\gamma_\alpha}{h_\alpha} \frac{\partial \phi}{\partial x_\alpha} \big) \Big) \tag{10}$$

Let us deal with the three-dimensional case. The region is divided into rectangular cells (control volumes), with ϕ discretized at cell centers. Consider an interior mesh point P, and integrate the differential equation over the control volume surrounding P. Denote the neighbours of P by E, W, N, S, T, B (east, west, north, south, top, bottom), and the corresponding cell faces by subscripts e, w, n, s, t, b. The volume integral is expressed as a sum of six surface integrals, e.g. for the 'east' face:

$$J_e = \iint (\rho u_1 \phi - \frac{\gamma_1}{h_1} \frac{\partial \phi}{\partial x_1}) h_2 h_3 \, dx_2 dx_3 \tag{11}$$

This expression will be approximated by

$$J_e \simeq \beta \phi_E - \alpha \phi_P \tag{12}$$

where the coefficients α and β depend on the strength of flow F_e and the conductance D_e:

$$
\begin{aligned}
F_e &= \iint \rho u_1 h_2 h_3 \, dx_2 dx_3 \\
D_e &= \frac{1}{d_e} \iint \gamma_1 h_2 h_3 \, dx_2 dx_3
\end{aligned}
\tag{13}
$$

where d_e is the distance between points P and E.

In the context of a discretization scheme one requires only approximate values of d_e, F_e, and D_e. So let A_e denote an approximate area of the cell face, and let h_1, ρu_1, and γ_1 stand for some local average of the corresponding continuous quantity, then $d_e \simeq h_1(x_1(E) - x_1(P))$, $F_e \simeq \rho u_1 A_e$, and $D_e \simeq \gamma_1 A_e / d_e$.

Two often used discretization schemes are the central difference scheme, which employs

$$
\alpha = -D_e - F_e/2, \qquad \beta = -D_e + F_e/2 \tag{14}
$$

and the upwind scheme, for which

$$
\alpha = -D_e - \max(F_e, 0), \qquad \beta = -D_e + \min(F_e, 0) \tag{15}
$$

The central difference scheme is second-order accurate, but unstable at high cell Péclet number, $P_e = F_e/D_e$, whereas the upwind scheme is always stable, but only first-order accurate.

Through consideration of the exact solution to the one–dimensional convection–conduction equation with constant coefficients, Patankar [4] is led to define two intermediate schemes, both of which approximate central differencing at low cell Péclet number, and upwind differencing with zero diffusion at high cell P. These are the piecewise linear scheme,

$$
\alpha = \left\{ \begin{array}{l} 0 \\ -D_e - F_e/2 \\ -F_e \end{array} \right\} \quad \text{if} \quad \left\{ \begin{array}{l} F_e/2 \le -D_e \\ |F_e/2| < D_e \\ F_e/2 \ge D_e \end{array} \right\} \tag{16}
$$

and the power law scheme,

$$
\alpha = \left\{ \begin{array}{l} 0 \\ -D'_e - \max(F_e, 0) \\ -F_e \end{array} \right\} \quad \text{if} \quad \left\{ \begin{array}{l} F_e/10 \le -D_e \\ |F_e/10| < D_e \\ F_e/10 \ge D_e \end{array} \right\} \tag{17}
$$

where $D'_e = D_e \, (1 - |P_e|/10)^5$. For all schemes, $\beta = \alpha + F_e$ and $\beta(D_e, F_e) = \alpha(D_e, -F_e)$

The power law scheme is employed in our code, although the piecewise linear scheme would serve just as well.

Relaxation procedure. In order to obtain a steady solution to the system of equations (1)–(5), a procedure is employed in which each equation is relaxed in turn, in a cyclic order until convergence is achieved. (For reasons to be discussed later, instead of (5) we employ the total energy equation, (4) + (5).) Time-stepping is employed, but only to obtain some under-relaxation; the discretization is fully implicit, and within any single timestep the equations are not relaxed to convergence. Each cycle consists of the following actions:

(a) The source terms S_n, S_{mu}, and $S_E^{e,i}$ are computed.

(b) The momentum balance equation (2) is relaxed by changes to the field u. Also the coefficient c_x is computed for each point in the mesh.

(c) v is adjusted to satisfy the diffusion equation (3), and the coefficients c_y are computed.

(d) The continuity equation (1) is relaxed and the equation of state is satisfied through simultaneous changes to n_i, u, v, and p.

(e) The ion energy equation (5) is relaxed by changes to the field T_i; the pressure is adjusted accordingly.

(f) The total energy equation, (4) + (5), is relaxed by changes to the field T_e; the pressure is adjusted accordingly.

Each of the five-point equations is relaxed by means of one or two iterations of the Strongly Implicit Procedure of Stone [**6**], as implemented in the NAG library code D03UAF [**9**]. The residuals of all equations are monitored in order to decide whether a converged solution has been achieved.

A special complication in the system (1)–(5) is the presence of two energy equations, which, due to the term $K_{ei}(T_e - T_i)$, may be strongly coupled, at least over part of the domain. To relax these equations separately would lead to very slow convergence. (Analogous problems occur in the modelling of chemically reacting flow). Our treatment, employing the sum equation and the ion-energy equation, eliminates this problem. An alternative is to employ the sum equation and the difference, but that is less satisfactory in the common case where the electron energy transport is dominant; then the sum and difference equations become strongly coupled.

3. An Example Calculation

Some early calculations with the code were presented in [**3**]. More recently the code was used, in collaboration with C.E. Singer, to provide predictions for the edge plasma in the proposed TFCX experiment at Princeton. Those studies are summarized in [**10**]. Shown here are the results of one particular calculation; the 'baseline case' of [**10**]. The present discussion refers to the equations as given in the appendix.

Geometry and boundary conditions. Fig. 1 shows a poloidal cross-section of the TFCX design, with the domain of the calculation indicated. This region is mapped to

the rectangular mesh as shown in Fig. 2. The size of this region is $4.0\,\mathrm{m} \times 0.2\,\mathrm{m}$, divided into 20×16 cells. It is to be noted that, although the parallel length scale is much larger than the perpendicular scale, also parallel transport coefficients are much larger than perpendicular ones, so the problem really is two-dimensional. The metric coefficients $\sqrt{g}$, h_x and h_y are constants in this calculation; $B_\theta/B = 0.2$.

The boundary conditions are the following:

– On the 'south' edge (the interface with the bulk plasma), the ion density and the parallel flow velocity were prescribed, $n_i = 10^{20}/\mathrm{m}^3$ and $u_\parallel = 0$. The conditions for the energy equations were $T_e = T_i = T_{bulk}$, but T_{bulk} was to be found as part of the overall solution process in order to obtain a prescribed average energy flux into the boundary plasma of $135\,\mathrm{kW/m^2}$.

– On the 'north' edge (the outer wall), we prescribed zero transverse particle flux, zero shear, and low values (2 eV) for T_e and T_i. (Note: in [**10**] actually, instead of zero particle flux, a fixed low value for the density was specified. Either condition is arbitrary to some extent).

– On the 'west' edge (the midplane), symmetry conditions were specified: zero parallel flow and zero parallel gradients of n_i, T_e and T_i.

– On the 'southern' half of the 'east' edge, again symmetry conditions were specified (but the density gradient was not fixed; we are only allowed three conditions here).

– On the 'northern' half of the 'east' edge (the limiter), sonic flow is required: $u_\parallel = \sqrt{p/\rho}$. Furthermore the energy fluxes are specified in the following form:

$$
\begin{aligned}
Q_e &= \delta_e n_e u T_e \\
Q_i &= \delta_i n_i u T_i + \frac{1}{2}\rho u u_\parallel^2
\end{aligned}
\tag{18}
$$

with $\delta_e = 4.0$ and $\delta_i = 2.5$; essentially this condition specifies the ratio between conducted and convected energy transport.

Model for atomic processes. The physical picture here [**1**] is that plasma striking the limiter is almost all released as neutral particles and re-ionized somewhere in the plasma volume, mainly very close to the limiter. (There is therefore almost no net plasma flow into the boundary region). An energy loss is associated with this re-ionization.

A proper treatment of these processes is beyond the scope of the present code; a Monte Carlo neutrals routine would be required. Instead we employ a crude but reasonable model for the recycling process, which conserves particles and approximates the proper energy loss terms. It is not neccessary to present the details here.

Transport coefficients. The coefficients $\eta_\parallel^i$, $\kappa_\parallel^e$, $\kappa_\parallel^i$ and K_{ei} are assumed classical. The radial transport coefficients were assigned anomalous values: $D = 2.5\,\mathrm{m^2/s}$, $\eta_y^i/\rho = 0.2\,\mathrm{m^2/s}$, $\kappa_y^e/n_e = 5\,\mathrm{m^2/s}$ and $\kappa_y^i/n_i = 0.2\,\mathrm{m^2/s}$.

Results. The outcome of this calculation is displayed in the contour plots, figs. 3–5.

Fig. 3 shows the density field n_i. In the narrow recycling zone in front of the limiter the density rises by a factor of six over the prescribed value at the interface with the bulk plasma, to a value $6 \times 10^{20}/\mathrm{m}^3$.

Fig. 4 shows the electron temperature T_e. Outside the recycling zone the strong parallel conductivity causes the temperature to be nearly constant along the fieldlines, but in front of the limiter T_e falls off rapidly. The expected temperature near material surfaces is a major engineering concern for the design of this type of experiment.

In fig. 5 the mach number of the parallel flow velocity is displayed. The direction of flow is to the left, away from the limiter, in the lower part of the domain, and towards the limiter in the upper part. The interest of this result is to bring out that the very localized recycling process does have a global influence on the flow field.

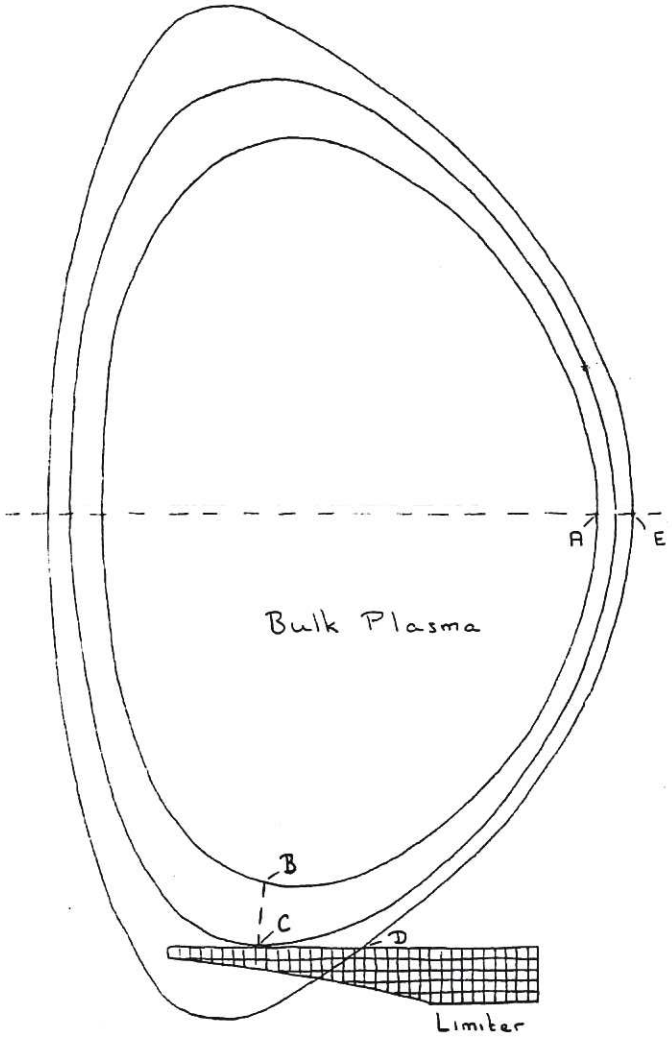

Fig. 1 Poloidal cross-section of the proposed TFCX experiment.
Points A–E show the boundary of the computational region.

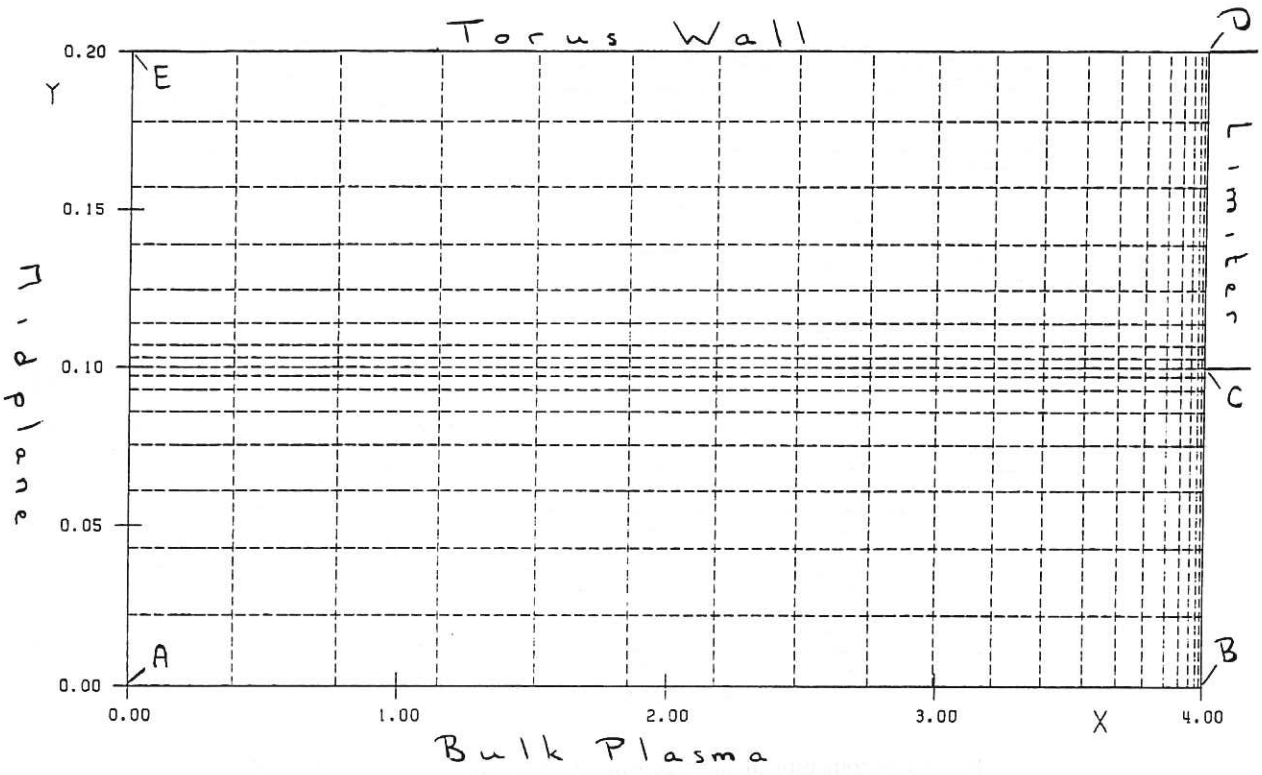

Fig.2 The computational mesh.

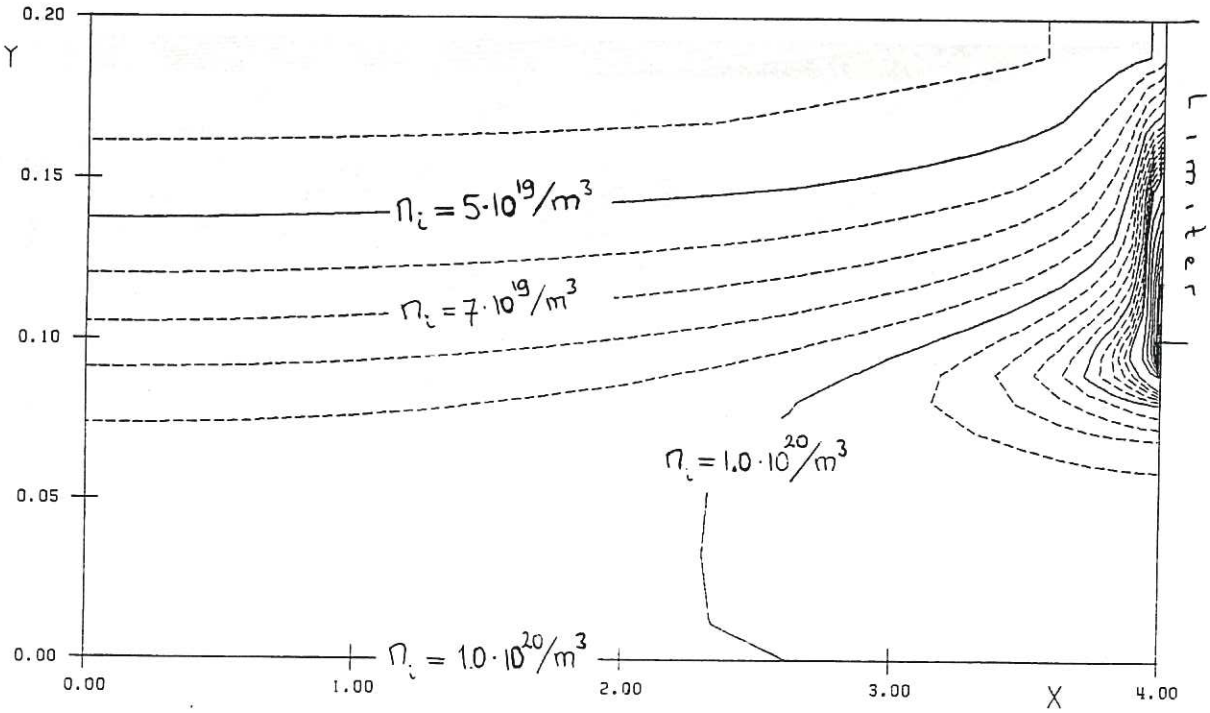

Fig.3 Contour plot of the ion density. The increment between the dotted contours is $1 \times 10^{19}/m^3$; between the solid contours it is $5 \times 10^{19}/m^3$.

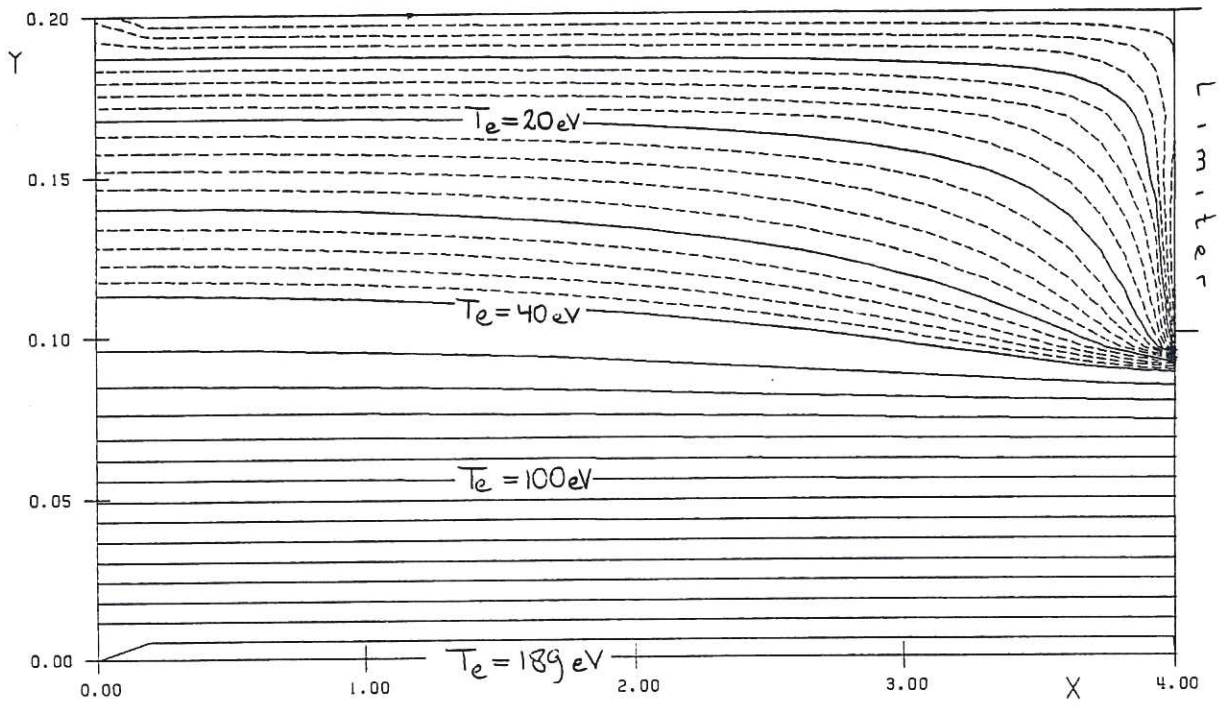

Fig.4 Contour plot of the electron temperature. The increments are 2eV between the dotted contours and 10eV between the solid contours.

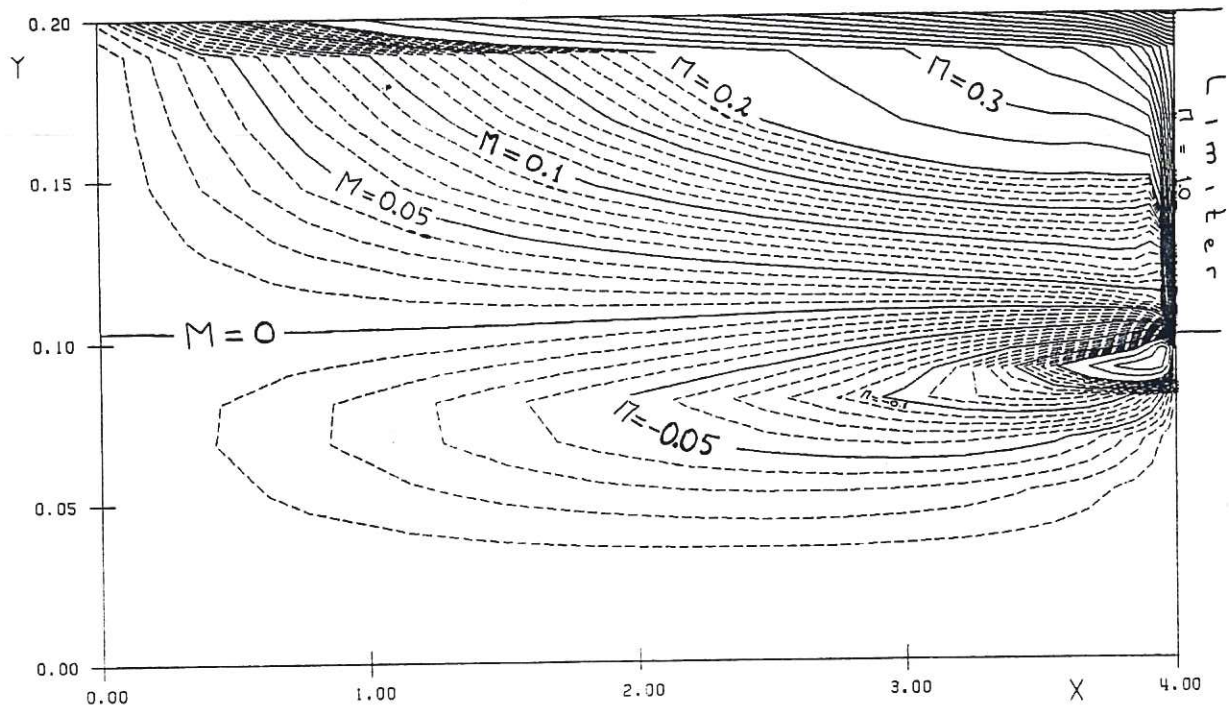

Fig.5 Contour plot of the Mach number. The increments are 0.01 between the dotted contours and 0.05 between the solid contours.

APPENDIX A. THE COMPLETE SET OF EQUATIONS

We employ a system of equations governing the ion density n_i, the parallel flow velocity $u_\parallel$, the radial diffusion velocity v, and electron- and ion temperatures T_e and T_i. Auxiliary physical quantities are the electron density, $n_e = Z_i n_i$, the mass density, $\rho = m_i n_i$, the total and partial pressures, $p = p_e + p_i = n_e T_e + n_i T_i$, and the poloidal flow velocity, $u = (B_\theta/B)u_\parallel$. The coordinates x and y correspond to the poloidal and radial directions respectively. $\sqrt{g}$, h_x and h_y are metric coefficients; the coordinate system may be curvilinear, although it must be orthogonal. The equations are:

$$\frac{\partial}{\partial t}n_i + \frac{1}{\sqrt{g}}\frac{\partial}{\partial x}\left(\frac{\sqrt{g}}{h_x}n_i u\right) + \frac{1}{\sqrt{g}}\frac{\partial}{\partial y}\left(\frac{\sqrt{g}}{h_y}n_i v\right) = S_n \tag{A.1}$$

$$\begin{aligned}\frac{\partial}{\partial t}(\rho u_\parallel) &+ \frac{1}{\sqrt{g}}\frac{\partial}{\partial x}\left(\frac{\sqrt{g}}{h_x}\rho u u_\parallel - \frac{\sqrt{g}}{h_x^2}\eta_x^i\frac{\partial u_\parallel}{\partial x}\right)\\ &+ \frac{1}{\sqrt{g}}\frac{\partial}{\partial y}\left(\frac{\sqrt{g}}{h_y}\rho v u_\parallel - \frac{\sqrt{g}}{h_y^2}\eta_y^i\frac{\partial u_\parallel}{\partial y}\right) = S_{mu_\parallel} - \frac{B_\theta}{B}\frac{1}{h_x}\frac{\partial p}{\partial x}\end{aligned} \tag{A.2}$$

$$v = -\frac{D}{h_y}\frac{\partial}{\partial y}(\ln n_i) \tag{A.3}$$

$$\begin{aligned}\frac{\partial}{\partial t}\left(\frac{3}{2}n_e T_e\right) &+ \frac{1}{\sqrt{g}}\frac{\partial}{\partial x}\left(\frac{\sqrt{g}}{h_x}\frac{5}{2}n_e u T_e - \frac{\sqrt{g}}{h_x^2}\kappa_x^e\frac{\partial T_e}{\partial x}\right)\\ &+ \frac{1}{\sqrt{g}}\frac{\partial}{\partial y}\left(\frac{\sqrt{g}}{h_y}\frac{5}{2}n_e v T_e - \frac{\sqrt{g}}{h_y^2}\kappa_y^e\frac{\partial T_e}{\partial y}\right)\\ &= S_E^e - K_{ei}(T_e - T_i) + \frac{u}{h_x}\frac{\partial p_e}{\partial x} + \frac{v}{h_y}\frac{\partial p_e}{\partial y}\end{aligned} \tag{A.4}$$

$$\begin{aligned}\frac{\partial}{\partial t}\left(\frac{3}{2}n_i T_i + \frac{1}{2}\rho u_\parallel^2\right)&\\ &+ \frac{1}{\sqrt{g}}\frac{\partial}{\partial x}\left(\frac{\sqrt{g}}{h_x}\left(\frac{5}{2}n_i u T_i + \frac{1}{2}\rho u u_\parallel^2\right) - \frac{\sqrt{g}}{h_x^2}\left(\kappa_x^i\frac{\partial T_i}{\partial x} + \frac{1}{2}\eta_x^i\frac{\partial u_\parallel^2}{\partial x}\right)\right)\\ &+ \frac{1}{\sqrt{g}}\frac{\partial}{\partial y}\left(\frac{\sqrt{g}}{h_y}\left(\frac{5}{2}n_i v T_i + \frac{1}{2}\rho v u_\parallel^2\right) - \frac{\sqrt{g}}{h_y^2}\left(\kappa_y^i\frac{\partial T_i}{\partial y} + \frac{1}{2}\eta_y^i\frac{\partial u_\parallel^2}{\partial y}\right)\right)\\ &= S_E^i + K_{ei}(T_e - T_i) - \frac{u}{h_x}\frac{\partial p_e}{\partial x} - \frac{v}{h_y}\frac{\partial p_e}{\partial y}\end{aligned} \tag{A.5}$$

S_n, $S_{mu_\parallel}$, S_E^e and S_E^i are volume sources of ions, momentum, electron and ion energy. η_x^i and η_y^i are the poloidal and radial ion viscosity coefficients; $\kappa_x^{e,i}$ and $\kappa_y^{e,i}$ are thermal conductivities. The poloidal coefficients are related to classical parallel coefficients according to $\eta_x^i = (B_\theta^2/B^2)\,\eta_\parallel^i$, and similarly for $\kappa_x^{e,i}$. The radial coefficients, including D, are anomalous. $K_{ei}(T_e - T_i)$ is the electron-ion energy equilibration term, and the

$\mathbf{u} \cdot \mathbf{grad}\, p_e$ term on the right hand side of the energy equations represents work done by the electric field.

ACKNOWLEDGEMENTS

This work would not have been possible without the Euratom mobility support, which enabled me to work first at UKAEA Culham laboratory and subsequently at IPP Garching. I am indebted to Prof. F. Engelmann, to M.F.A. Harrison and the Exhaust Physics Group at Culham, and to K. Lackner and the Tokamak Physics Group at IPP for many fruitful discussions. This work was performed under the Euratom–FOM association agreement with financial support from ZWO and Euratom.

REFERENCES

1. M.F.A. Harrison, *Boundary Plasma*, in "Applied Atomic Collision Physics", Edited by H.S.W. Massey, B. Bederson and E.W. McDaniel, Academic Press, New York, 1983.
2. B.J. Braams, *Numerical Studies of the Two-Dimensional Scrapeoff Plasma*, Presented at the 11th European Conference on Controlled Fusion and Plasma Physics, Aachen, 1983, Europhysics Conference Abstracts 7D–II (1983), 431–434.
3. B.J. Braams, P.J. Harbour, M.F.A. Harrison, E.S. Hotston and J.G. Morgan, *Modelling of the Boundary Plasma of Large Tokamaks*, J. Nucl. Mater. **121** (1984), 75–81.
4. S.V. Patankar, "Numerical Heat Transfer and Fluid Flow", Hemisphere, New York, 1980.
5. S.V. Patankar and D.B. Spalding, *A Calculation Procedure for Heat, Mass and Momentum Transfer in Three-Dimensional Parabolic Flows*, Int.J.Heat Mass Transfer **15** (1972), 1787–1806.
6. H.J. Stone, *Iterative Solution of Implicit Approximations of Multi-Dimensional Partial Differential Equations*, SIAM J.Numer.Anal. **5** (1968), 530–558.
7. P.J. Roache, "Computational Fluid Dynamics", 2nd ed., Hermosa, 1976.
8. A. Brandt, *Guide to Multigrid Development*, in "Multigrid Methods", Proceedings of the Conference held at Köln–Porz, Nov. 1981 (W. Hackbusch, U. Trottenberg, eds.). Lecture Notes in Mathematics., Springer, Berlin, 1982.
9. Numerical Algorithms Group, "NAG Fortran Manual for Mark 10", NAG, Oxford, 1983.
10. C.E. Singer and B.J. Braams, *Low Temperature Plasma near a Limiter — A Solution for the Tokamak Fusion Core Experiment*, Applied Physics Division Report No. 30, Princeton Plasma Physics Laboratory, 1984. (to be published).